Volume 1 | Number 1 | Jan 2013 | Pages 1–100

ChemComm

Chemical Communications
www.rsc.org/chemcomm

ROYAL SOCIETY OF CHEMISTRY

This is an *Accepted Manuscript*, which has been through the Royal Society of Chemistry peer review process and has been accepted for publication.

Accepted Manuscripts are published online shortly after acceptance, before technical editing, formatting and proof reading. Using this free service, authors can make their results available to the community, in citable form, before we publish the edited article. We will replace this *Accepted Manuscript* with the edited and formatted *Advance Article* as soon as it is available.

You can find more information about *Accepted Manuscripts* in the **Information for Authors**.

Please note that technical editing may introduce minor changes to the text and/or graphics, which may alter content. The journal's standard **Terms & Conditions** and the **Ethical guidelines** still apply. In no event shall the Royal Society of Chemistry be held responsible for any errors or omissions in this *Accepted Manuscript* or any consequences arising from the use of any information it contains.

www.rsc.org/chemcomm

Journal Name

COMMUNICATION

Electrocatalytic hydrogen generation by a trithiolato-bridged dimanganese hexacarbonyl anion with turnover frequency exceeding 40,000 s^{-1}

Kaipeng Hou, Hwa Tiong Poh and Wai Yip Fan*

An unusual ionic manganese model complex [Mn(bpy)$_3$]$^+$[(CO)$_3$Mn(μ-SPh)$_3$Mn(CO)$_3$]$^-$(bpy: 2,2′-bipyridine) has been synthesized, which bears some structural resemblance to the active site of [FeFe] hydrogenase. An overpotential of 0.61V has been determined for the electrocatalytic proton reduction using this complex in CH$_3$CN with CF$_3$COOH as the proton source. A turnover frequency of 44600 s^{-1} is achieved at high scan rates and in the presence of a large amount of acid.

Hydrogenase enzymes are divided into three types according to the different metals in the active sites: [NiFe], [FeFe] and [Fe]only.[1] The former two can catalyze reversible proton reduction to molecular hydrogen at low overpotentials with remarkable efficiency.[2] In the [FeFe] hydrogenase, the two iron centres bearing CO and CN ligands are bridged by a unique azadithiolate ligand for which the nitrogen atom serves as the protonation site during proton reduction.[3]. The reduction is assumed to be a 2e$^-$ process where the 2Fe2S core provides one electron with the second electron supplied by the [Fe4S4] cluster (Scheme 1).[4]

There have been many studies of synthetic [FeFe] hydrogenase models based on the μ^2-dithiolato-bridged diiron moiety (μ^2-RS)$_2$Fe$_2$ coordinated to a variety of ligands such as CO, amines and phosphines. Several reviews have resulted from extensive studies of their structures, infrared spectroscopy and proton reduction efficiencies with acetic acid or trifluoroacetic acid as proton sources.[5-7] Recently, a Ni/Mn model complex has been synthesized whereby an azadiphosphine (Ph$_2$P)$_2$NR-chelated nickel center was linked to manganese by two thiolate ligands.[8] The Artero group introduced a dinuclear Ni/Mn complex as a bio-inspired mimic of the active site of [NiFe] hydrogenases catalyzing hydrogen evolution from trifluoroacetic acid with an overpotential 0.86 V.[9] Although many thiolate-bridged dimanganese complexes have been prepared, no studies on their proton reduction catalytic efficiencies have been reported. Furthermore the many different oxidation states exhibited by manganese should enable redox reactions to be carried out in a facile manner.

In this work, we will show that a μ_3-thiolato dimanganese hexacarbonyl anion, Mn$_2$(SPh)$_3$(CO)$_6^-$ (complex **1** in Scheme 1), which structurally resembles the active site of [FeFe] hydrogenase, can catalyze electrochemical proton reduction with low overpotential coupled with very high turnover rates. We will also present a mechanism based on the experimental results.
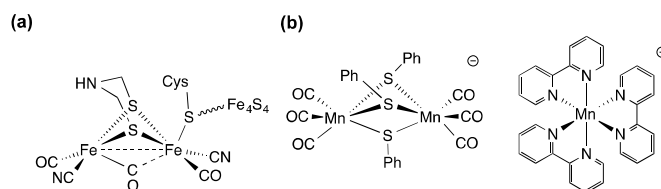
Scheme 1. (a) Active site of [FeFe] hydrogenase and (b) model complex 1 of this work

Complex **1** is synthesized via a one-pot uv photolysis of Mn$_2$(CO)$_{10}$, diphenyl disulfide and 2,2′-bipyridine for 2 hours. An alternative pathway to **1** is also carried out whereby Mn$_2$(CO)$_{10}$ and diphenyl disulfide are uv-irradiated to first form the dithiolato-bridged complex [Mn(CO)$_4$(μ-SPh)]$_2$. This complex is further irradiated in the presence of 2,2′-bipyridine to generate **1**. Suitable crystals of **1** are grown in acetone solvent and stored at low temperature before being subjected to X-ray diffraction.
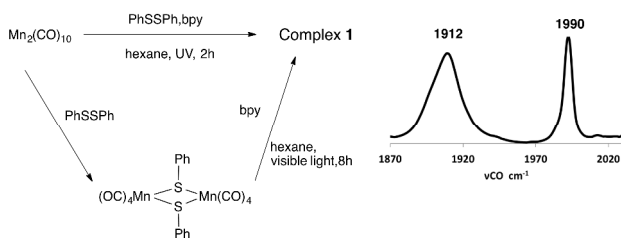

Figure 1. Two pathways to form complex **1** and the vCO IR spectra of complex **1** in CH$_3$CN.

Complex **1** consists of a dinuclear manganese anion and a mono-manganese cation (Figure 1). The anionic part is [(CO)$_3$Mn(μ-SPh)$_3$Mn(CO)$_3$]$^-$, which contains two manganese(I), each

coordinated by three terminal CO ligands and bridged by three μ-SPh ligands. The phenyl groups are not coplanar due to steric repulsion but instead form a propeller-like arrangement. The distance between the two Mn atoms is 3.1646(10) Å which is too long for a Mn-Mn single bond.[10] The IR spectra of complex **1** show two strong v_{CO} absorptions at 1910 and 1992 cm^{-1} whose patterns are indicative of C_{3v} symmetry around each of the Mn centre. The Mn(I) center in Mn(bpy)$_3$$^+$ cation is coordinated by three bidentate bipyridine ligands, resulting in a highly-distorted octahedral geometry. The Mn-N bond lengths range from 2.236(4) to 2.263(4) Å, which are similar to those reported for Mn(II) octahedral tris(2,2′-bipyridine) complexes.[11]
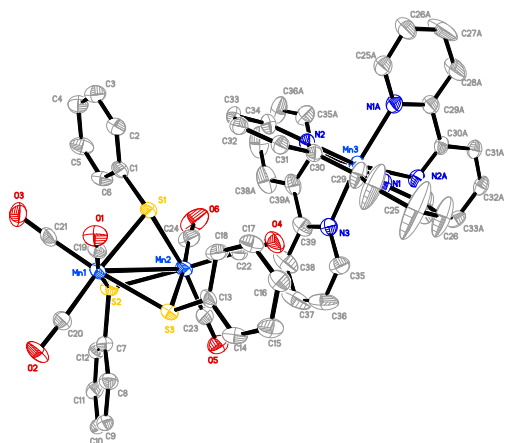

Figure 2. ORTEP view of solid-state structure of **1**. Hydrogen atoms are omitted for clarity.

The route to the formation of **1** is complicated. Successive nucleophilic substitution of the Mn$_2$(CO)$_8$(SPh)$_2$ dimer by 2,2′-bipyridine will eventually afford Mn(bpy)$_3$$^+$ and PhS$^-$. The thiolate ion then reacts with the dimer to generate Mn$_2$(CO)$_3$(SPh)$_3$$^-$ upon dissociation of two Mn-CO bonds.

The cyclic voltammetric diagram of 1 in the absence of acid shows a small reduction peak at -1.90 V (vs Fc$^+$/Fc in CH$_3$CN), which correspond to the reduction of the Mn(bpy)$_3$$^+$ cation respectively (Figure 3). The assignment is based on a previous study on the reduction potentials of Mn(I) to Mn(0) bipyridine complexes.[12] As the addition of trifluoroacetic acid (TFA) causes the peak intensity to increase as well, it would appear the cation itself is able to catalyze proton reduction albeit at a relatively high overpotential of 1.01 V (TFA reduction in CH$_3$CN occurs at -0.89 V vs Fc$^+$/Fc). Another smaller reduction peak is observed at -1.50 V, which we have attributed to the reduction of the anion. Interestingly this peak appears to have shifted to -1.20 V upon acid addition and remains at constant height independent of the acid concentration. We believe that protonation of the anion has taken place and hence reduces its reduction potential, as opposed to the higher charge repulsion between the anion and electron in the absence of acid. At the same time a large peak which grows with acid addition is observed at -1.50 V to -1.60 V depending on the acid concentration.[8] The potential at -1.50 V is attributed to the catalytic proton reduction potential of the anion, which corresponds to an overpotential of 0.61 V. The electrocatalytic H$_2$ production was further confirmed by bulk

electrolysis of **1** with excessive CF$_3$COOH in CH$_3$CN at -1.50 V vs Fc$^+$/Fc with consistently more than 75% Faraday yield.

The catalytic rate of proton reduction is investigated next. To estimate the rate, an approximate model for pseudo-first-order catalytic systems previously used before is adopted here, as shown by the following equation.[13]

$$\frac{i_c}{i_p} = \frac{n}{0.446}\sqrt{\frac{RTk_{obs}}{F\upsilon}}$$

i_c is the catalytic current, i_p is the peak current measured in the absence of acid, n is the number of electrons involved in the catalytic reaction, k_{obs} is the observed first-order rate constant, R is the ideal gas constant, T is the temperature in Kelvin, F is Faraday's constant, υ is the scan rate. From our data (Figure 3b), k_{obs} increases linearly with acid concentration, which suggests a first-order dependence of the catalytic rate on acid concentration. At the highest concentration of CF$_3$COOH (300 mM) studied, a $\frac{i_c}{i_p}$ value of 152 was obtained, which corresponds to a turnover frequency of 44600 s^{-1} at 295 K.
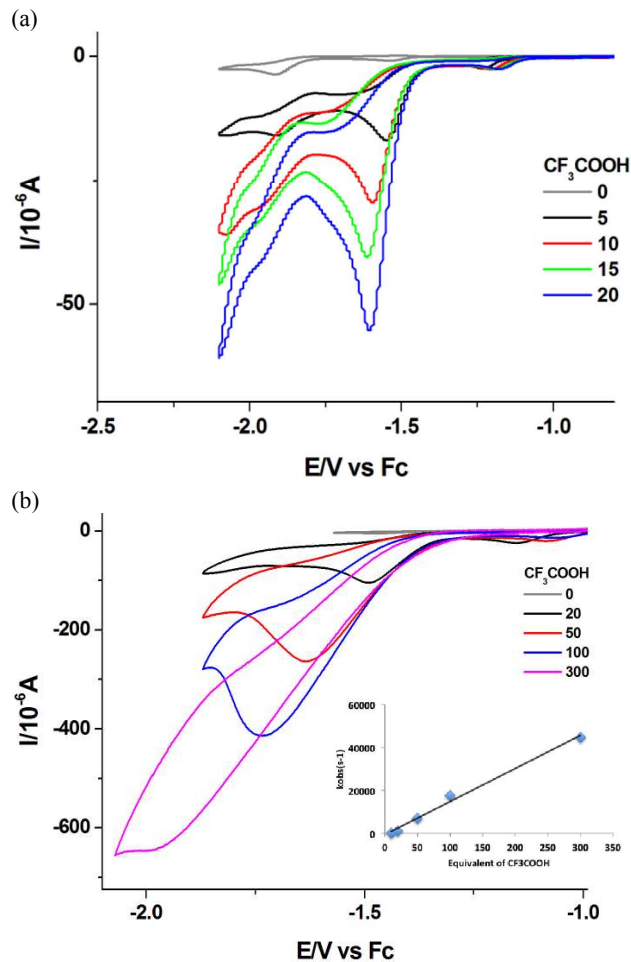
(a)

(b)

Figure 3. (a) Cyclic voltammograms of **1** (1.0 mM) with TFA (0−20 mM) in 0.1 M Bu$_4$NPF$_6$ in CH$_3$CN at a scan rate of 0.1 V/ sec. (b) Cyclic voltammograms of 1 (1.0 mM) with TFA (0−300 mM) in 0.1 M Bu$_4$NPF$_6$ in CH$_3$CN at a scan rate of 1 V/ sec. k_{obs} relationship

with acid increasing concentration (inset graph). 1 mm glassy-carbon working electrode, platinum counter electrode at 295 K.

From the CV measurements, the anion appears to play a more important role in reducing the overpotential of proton reduction, hence the anion-catalysed mechanism is studied in more detail here. From the sequence of the process, the proton reduction mechanism catalyzed by **1** is proposed to be a CECE (chemical-electrochemical-chemical-electrochemical) process similar to iron and nickel model complexes (Figure 4). The anion is first protonated to form intermediate **1H⁺**. Then **1H⁺** is reduced at -1.2 V vs Fc⁺/Fc to generate a hydride species **1H** by an intrahydride transfer from sulfur to manganese.[14] A second proton reacts with **1H** to generate **1H₂**. Finally, dihydrogen is released and the anion is regenerated upon electron reduction at -1.5V vs Fc⁺/Fc to complete the catalytic cycle.

To lend more insight into the mechanism, the reactivity and stability of **1** in the presence of acids are first studied via infrared spectroscopy. When one equivalent CF_3COOH is added to **1** in CH_3CN, no change in the ν_{CO} peaks is observed even after an hour. However, when the amount of acid is increased to 50 equivalence, the initial peaks of **1** at 1910 cm⁻¹ and 1992 cm⁻¹ slowly decrease while two new peaks at 1932 cm⁻¹ and 2015 cm⁻¹ appear. Based on a literature search, we are able to assign the 1932 and 2015 cm⁻¹ bands to the manganese carbonyl tetramer $Mn_4(CO)_{12}(SPh)_4$.[15]
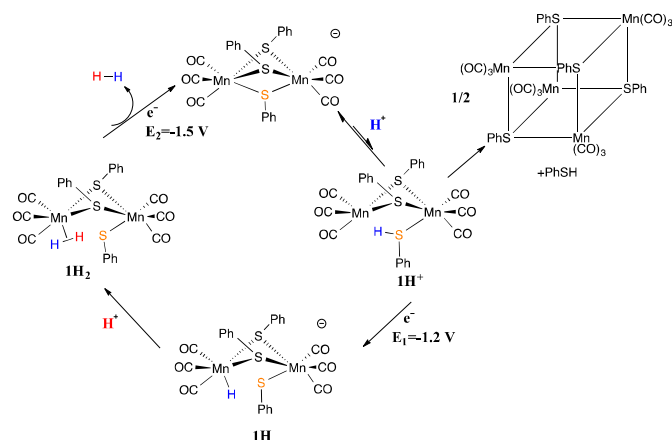

Figure 4. Proposed mechanism for proton reduction process based on experimental results.

The study indicates that **1** is moderately stable under acidic conditions, at least within the period when cyclic voltammetric studies were carried out. Hence the redox processes under different acid concentrations are due to **1** rather than to the intermediates formed upon acidification. The tetrameric manganese cluster is probably formed from the dimerization of intermediate **1H⁺** upon the dissociation of its benzenethiol ligand. Hence the tetramer formation may represent a competing reaction step for the reduction of intermediate **1H⁺** to **1H**. However, our experimental data suggest that **1H⁺** is relatively stable since the formation of the manganese tetramer is shown to be sluggish which in turn enables a high proton reduction catalytic rate to be achieved.

Although the overpotentials of many [FeFe] hydrogenase model complexes such as the diiron dithiolato bridged complexes fall within 0.2 V and 1.1 V, very few complexes actually exhibited overpotentials smaller than 0.6V.[5] However complexes with low overpotentials are also less efficient in generating large proton reduction currents. The TOF for proton reduction catalysed by a diiron complex[16] can reach 58000 s⁻¹ while the highest TOF reported

for a nickel complex in dry and wet CH_3CN were 33000 s⁻¹ and 106000s⁻¹ respectively with an overpotential of 0.625V.[13,14] A comparison with these iron and nickel models shows that complex **1** is indeed a fairly efficient catalyst for proton reduction with an overpotential of 0.61V. However if the homoconjugation effect of TFA is considered, the overpotential would become 0.79V while Helm's method would give a value of 0.69V.[17,18]

In summary, we have shown that a manganese complex, which is structurally similar to the active site of [FeFe] hydrogenase, can catalyze proton reduction with high TOF. The unusual structure of complex **1** contains a dinuclear manganese anion bridged by three μ-SPh groups and a mono-manganese cation where Mn(I) is coordinated by three 2,2′-bipyridine ligands. A simple mechanism showing how proton reduction takes place electrochemically is also proposed. We have demonstrated that manganese-only model complex can also catalyze proton reduction at least as efficient as some iron or nickel model complexes.

Notes and references

1 Evans, D. J.; Pickett, C. J. *Chem. Soc. Rev.* 2003, **32**, 268.
2 De Lacey, A. L.; Fernández, V. M.; Rousset, M.; Cammack, R. *Chem.Rev.*, 2007, **107**, 4304.
3 Appel, A. M.; Bercaw, J. E.; Bocarsly, A. B.; Dobbek, H.; DuBois, D. L.; Dupuis, M.; Ferry, J. G.; Fujita, E.; Hille, R.; Kenis, P. J. A. *Chem. Rev.*, 2013, **113**, 6621
4 Gloaguen, F.; Rauchfuss, T. B. *Chem. Soc. Rev.*, 2009, **38**, 100.
5 Felton, G. A. N.; Mebi, C. A.; Petro, B. J.; Vannucci, A. K.; Evans, D. H.; Glass, R. S.; Lichtenberger, D. L. *J. Organomet. Chem.*, 2009, **694**, 2681.
6 Capon, J.-F.; Gloaguen, F.; Pétillon, F. Y.; Schollhammer, P.; Talarmin, J. *Coord. Chem. Rev.*, 2009, **253**, 1476.
7 Tard, C.; Pickett, C. J. *Chem. Rev.*,2009, **109**, 2245.
8 Song, L.-C.; Li, J.-P.; Xie, Z.-J.; Song, H.-B. *Inorg.Chem.*, 2013, **52**, 11618.
9 Fourmond, V.; Canaguier, S.; Golly, B.; Field, M. J.; Fontecave, M.; Artero, V. *Energy Environ. Sci.*, 2011, **4**, 2417.
10 McDonald, J. W. *Inorg. Chem.*, 1985, **24**, 1734.
11 Yu, X.-L.; Tong, Y.-X.; Chen, X.-M.; Mak, T. C. W. *J. Chem. Crystallogr.*, 1997, **27**, 441.
12 Wang, M.; England, J.; Weyhermüller, T.; Wieghardt, K. *Inorg. Chem.*, 2014, **53**, 2276.
13 Helm, M. L.; Stewart, M. P.; Bullock, R. M.; DuBois, M. R.; DuBois, D. L. *Science.*, 2011, **333**, 863.
14 Dupuis, M.; Chen, S.; Raugei, S.; DuBois, D. L.; Bullock, R. M. *J. Phys. Chem. A*, 2011, **115**, 4861.
15 Reyes-Lezama, M.; Toscano, R. A; N. Zuñiga-Villareal, *J. Organomet. Chem.*, 1996, **517**, 19.
16 Carroll, M. E.; Barton, B. E.; Rauchfuss, T. B.; Carroll, P. J. *J. Am. Chem. Soc.*, 2012, **134**, 18843.
17 Fourmond, V.; Jacques, P.-A.; Fontecave, M.; Artero, V. *Inorg Chem.*, 2010, **49**, 10338.
18 Appel, A. M.; Helm, M. L. *ACS Catal*. 2014, **4**, 630.